

Modulus weighting method for static stiffness estimations of suction caisson foundations in layered soil conditions

Stephen K. Suryasentana¹

Harvey J. Burd²

Byron W. Byrne³

Avi Shonberg⁴

Affiliations

¹ Department of Civil and Environmental Engineering, University of Strathclyde, Glasgow, UK;

stephen.suryasentana@strath.ac.uk (Orcid: 0000-0001-5460-5089)

² Department of Engineering Science, University of Oxford, Oxford, UK;

harvey.burd@eng.ox.ac.uk (Orcid: 0000-0002-8328-0786)

³ Department of Engineering Science, University of Oxford, Oxford, UK;

byron.byrne@eng.ox.ac.uk (Orcid: 0000-0002-9704-0767)

⁴ Ørsted Wind Power, London, UK

avish@orsted.com

Corresponding author information

Stephen K. Suryasentana

stephen.suryasentana@strath.ac.uk

Number of words in the main text (excluding abstract and references)

2218

Number of figures

8

Number of tables

6

Date

12 Dec 2022

Abstract

This paper presents a new approach, called the Modulus Weighting Method (MWM), for estimating the static stiffness of suction caisson foundations in layered soil conditions. The existing simplified design models for estimating caisson stiffness are limited to non-layered soil conditions, but layered conditions are often found in real-world scenarios. A three-dimensional (3D) finite element analysis (FEA) study was conducted to develop and validate the MWM approach, and the results showed that it performs well in comparison to the 3D FEA results while being much more computationally efficient.

Keywords

Stiffness, shallow foundations, foundations, soil/structure interaction

NOTATION

z	depth below ground level
D	foundation diameter
\bar{z}	normalized depth with respect to foundation diameter
V	vertical load applied to foundation
H	lateral load applied to foundation
M	rotational moment applied to foundation
Q	torsion applied to foundation
G	shear modulus of elastic half-space (soil)
E	Young's modulus of elastic half-space (soil) = $2G(1+\nu)$
ν	Poisson's ratio of elastic half-space (soil)
α	factor controlling the rate of increase of the shear modulus with depth
G_R	reference shear modulus value
G_{eq}	equivalent constant shear modulus value for a non-homogeneous elastic half-space
G_{eq}^{skirt}	equivalent constant shear modulus value for skirt soil reactions of a caisson
G_{eq}^{base}	equivalent constant shear modulus value for base soil reactions of a caisson
η^{skirt}	non-homogeneity factors for skirt soil reactions
G_{fac}	factored shear modulus, $\eta^{skirt}G$
w_σ	stress-based weight distribution
w_ε	strain-based weight distribution
K_V	vertical stiffness of the soil-foundation interaction
K_H	lateral stiffness of the soil-foundation interaction
K_M	rotational stiffness of the soil-foundation interaction
K_Q	torsional stiffness of the soil-foundation interaction
p_{atm}	atmospheric pressure

1 Introduction

Suction caisson, or suction bucket, foundations are an important option for offshore wind turbines (Byrne & Houlsby, 2003). For large-scale foundation design projects such as offshore wind farms, efficient design models are needed to estimate the caisson response for optimisation of hundreds of foundations. The static stiffness of the caisson response, in particular, has important applications such as natural frequency analysis. Doherty et al. (2005) and Efthymiou & Gazetas (2018) have proposed efficient macro-element models to estimate the static stiffness of the caisson response in homogeneous and non-homogeneous linear elastic soil. Similarly, Suryasentana et al. (2017, 2022) have recently proposed an efficient Winkler model to estimate the static stiffness of caissons under six degrees-of-freedom (6DoF) loading in homogeneous and non-homogeneous linear elastic soil. However, none of these existing design models provide a direct means of modelling layered soil conditions, which are commonplace in offshore wind sites (Burd et al. 2020). Therefore, it is important to have an efficient design model to estimate the static stiffness of caissons in layered soil conditions.

Previous research on estimating the static stiffness of foundations in layered soil conditions has primarily focused on pile foundations. Poulos (1979) proposed a solution for axially loaded piles that transforms a non-homogeneous soil system into a 'two-layer' system, with the first layer along the pile shaft and the second layer below the pile base. The first layer has a constant shear modulus equivalent to the average shear modulus along the pile shaft, while the second layer has a constant shear modulus equivalent to the average shear modulus from the base depth to 5 pile diameters length below the base. Recently, Suryasentana & Mayne (2022) proposed a 'work-equivalent' framework that can estimate the static stiffness of circular surface foundations in layered soil conditions, by transforming a non-homogeneous soil system into a homogeneous soil system with a constant shear modulus equivalent to some weighted average of the non-homogeneous (and potentially layered) shear modulus profile.

The current paper aims to extend the OxCaisson Winkler model proposed by Suryasentana et al. (2022) to estimate the static stiffness of suction caissons in layered soil conditions. This is done through a new design approach called the 'Modulus Weighting Method' (MWM), which follows the

approach of Poulos (1979) in transforming the non-homogeneous soil system into two layers: one along the caisson skirt and the other below the caisson base. Each layer has its own constant shear modulus that is based on a weighted average of the shear modulus profile. The weighting is determined using weight distribution functions that are calibrated using a 3D FEA study, following the framework of Suryasentana & Mayne (2022).

2 Weight distributions

The work-equivalent framework (Suryasentana & Mayne 2022) is an approach to convert any non-homogeneous linear elastic half-space into a homogeneous linear elastic half-space with a constant shear modulus G_{eq} . There are two ways to do the transformation, depending on the assumptions.

Assumption 1: There exists a ‘stress-based weight distribution’ w_σ that is approximately invariant to changes in the shear modulus profile.

Based on Assumption 1, G_{eq} is calculated as,

$$\frac{1}{G_{eq}} = \int_0^\infty \frac{1}{G} w_\sigma d\tilde{z} \quad (1)$$

where $\tilde{z} = z/D$, z is the depth below ground level and D is the foundation diameter.

Assumption 2: There exists a ‘strain-based weight distribution’ w_ε that is approximately invariant to changes in the shear modulus profile.

Based on Assumption 2, G_{eq} is calculated as,

$$G_{eq} = \int_0^\infty G w_\varepsilon d\tilde{z} \quad (2)$$

The 3D FEA results in Suryasentana & Mayne (2022) indicate that Assumption 1 is valid for circular surface foundations under 6DoF loading, but Assumption 2 is not valid. The current paper extends this work by assessing these assumptions for suction caissons under 6DoF loading.

OxCaisson represents the soil response using Winkler-type soil reactions, which consist of distributed 'skirt soil reactions' acting along the caisson skirt and concentrated 'base soil reactions' acting on the caisson base. The MWM approach transforms the non-homogeneous soil system into two homogeneous layers (see Fig. 1). The first layer has a constant shear modulus G_{eq}^{skirt} for calculating the skirt soil reactions. The second layer has a constant shear modulus G_{eq}^{base} for calculating the base soil reactions. Two separate G_{eq} were adopted here, instead of a single overall G_{eq} , as it is expected that the shear modulus values influencing the skirt soil reactions will be significantly different from those influencing the base soil reactions. MWM assumes that there exists two weight distributions that are approximately invariant to changes in the shear modulus profile and can be used to calculate G_{eq}^{skirt} and G_{eq}^{base} , respectively. A 3D FEA study is carried out to determine these two weight distributions.

3 3D finite element study

Following Suryasentana & Mayne (2022), a 3D FEA study was carried out using Abaqus v6.13 (Dassault Systèmes 2014) to assess Assumptions 1 and 2 for the caisson problem. The 3D FEA model in this study is the same as that described in Suryasentana et al. (2022) and is briefly described below. The 3D FEA model consists of a rigid caisson of diameter D embedded in non-homogeneous elastic soil with shear modulus profiles of the following form,

$$G = G_R \left(\frac{2z}{D} \right)^\alpha \quad (3)$$

where α is a parameter and G_R is a reference shear modulus. Several caisson lengths ($L/D = 0.125, 0.25, 0.5, 1, 2$) in various soil properties (Poisson's ratio $\nu = 0, 0.1, 0.2, 0.3, 0.4, 0.49$ and $\alpha = 0, 0.2, 0.4, 0.6, 0.8, 1$) are analysed. The soil is weightless and isotropic linear elastic. First-order brick elements C3D8 (or C3D8H for $\nu = 0.49$) are assigned to the soil elements. The mesh domain is set to $100D$ for both width and depth, as mesh sensitivity analysis indicated that increasing the mesh domain beyond $100D$ does not significantly affect the static stiffness calculations. An example 3D FEA mesh is shown in Fig. 4 of Suryasentana et al. (2022). The loading reference point (LRP) is set at the centre of its lid base (see Fig. 1). Contact breaking between the soil and caisson is prevented using tie constraints at the soil-caisson interface. This is considered a reasonable assumption as the current study is focused on static stiffness estimations at low load levels, where the soil deformation is

assumed to be within the elastic strain limit of 10^{-6} (Atkinson 2000). For small strains, contact between the soil and caisson is maintained due to the initial K_o (compressive) stresses in the soil. Due to symmetry, only four displacement modes (see Table 1) are prescribed to compute the caisson response for 6DoF loading.

Two types of analysis are carried out to determine the weight distributions for calculating G_{eq}^{skirt} and G_{eq}^{base} . For the first analysis, the tie constraints between the caisson base (including the soil plug) and the soil elements beneath it are removed. As a result, the untied soil elements do not directly resist the caisson, and the calculated base soil reactions will be zero. This means that the soil resistance on the caisson is due only to the skirt soil reactions. This enables the determination of the weight distributions for calculating G_{eq}^{skirt} . For the second analysis, the tie constraints between the caisson skirt exterior and the soil elements in contact with it are removed. The calculated skirt soil reactions will be zero and this enables the determination of the weight distributions for calculating G_{eq}^{base} . For both types of analysis, the weight distributions are determined from the elastic strain energy of the soil elements, following the procedures detailed in the appendix of Suryasentana & Mayne (2022).

3.1 Assessment of Assumptions 1 and 2

Figs. 2 and 3 compare the 3D FEA-calculated w_σ and w_ε weight distributions under the application of only the skirt and base soil reactions, respectively. Only the results for $L/D = 1$ are shown, but conclusions are similar for other L/D ratios. The figures show that only w_ε stays approximately invariant with α for the skirt soil reactions, while both w_σ and w_ε stays approximately invariant with α for the base soil reactions. This is surprising as Suryasentana & Mayne (2022) shows that only w_σ stays approximately invariant with α for a circular surface foundation (which is effectively the base soil reactions for a caisson with $L/D = 0$). This suggests that for the base soil reactions, the assumption that w_ε stays approximately invariant with α may not be valid as L/D approaches zero. Fig. 2 provides support for only Assumption 2 for the skirt soil reactions, while Fig. 3 provides support for both Assumptions 1 and 2 for the base soil reactions.

4 Modulus Weighting Method

MWM adopts Assumption 1 to calculate G_{eq}^{base} (for consistency with the results for $L/D = 0$) and Assumption 2 to calculate G_{eq}^{skirt} . Thus, G_{eq}^{base} and G_{eq}^{skirt} may be calculated using Eqs. 1 and 2, respectively. Similar to the approach of Poulos (1979), only the shear modulus below the caisson base is considered in the calculation for G_{eq}^{base} . Fig. 2 shows that w_ε tends to be uniform along the skirt length. For simplicity, the peak towards the caisson base is not modelled for the skirt soil reactions. Fig. 3 shows that w_σ decreases approximately exponentially below the caisson base. Thus, MWM adopts the exponential and uniform weight distribution functions to approximate w_σ and w_ε , respectively,

$$\hat{w}_\sigma = \begin{cases} \frac{1}{b} \exp\left[-\left(\frac{\bar{z} - L/D}{b}\right)\right] & \text{for } \bar{z} \geq L/D \\ 0 & \text{for } \bar{z} < L/D \end{cases} \quad (4)$$

$$\hat{w}_\varepsilon = \begin{cases} \frac{1}{m} & \text{for } 0 \leq \bar{z} \leq m \\ 0 & \text{for } \bar{z} < 0 \text{ or } \bar{z} > m \end{cases} \quad (5)$$

where b and m are parameters. Least squares regression is carried out to identify the optimal parameter values that best fit the true weight distributions calculated from 3D FEA.

Based on the regression results, the following approximating functions for b and m are obtained:

$$b = b_1 + b_2 v^{b_3} + b_4 L/D \quad (6)$$

$$m = (m_1 + m_2 v)(L/D)^{m_3} \quad (7)$$

where the best-fit coefficient values are listed in Tables 2 and 3. Figs. 2 and 3 also show the resultant weight distributions based on Eqs. 4 to 7 (labelled as w^{skirt} and w^{base} for the skirt and base soil reactions, respectively), which indicate that these weight distributions approximately capture the salient trends of the 3D FEA-calculated weight distributions.

Using a constant G_{eq}^{skirt} implies that the skirt soil reactions are constant along the caisson skirt, which is unrealistic. Thus, non-homogeneity factors η^{skirt} are derived such that the work done by a factored shear modulus $G_{fac}(z) = \eta^{skirt} G(z)$ is equal to the work done when G_{eq}^{skirt} is applied i.e.

$$\frac{1}{2} G_{\text{eq}}^{\text{skirt}} \int_0^L \bar{k}_0^{\text{skirt}} (\Delta s)^2 dz = \frac{1}{2} \int_0^L (\eta^{\text{skirt}} G(z)) \bar{k}_0^{\text{skirt}} (\Delta s)^2 dz \quad (8)$$

$$\eta^{\text{skirt}} = G_{\text{eq}}^{\text{skirt}} \frac{\int_0^L dz}{\int_0^L G(z) dz} = \frac{G_{\text{eq}}^{\text{skirt}}}{G_{\text{sk}}} \quad (9)$$

where G_{sk} is the average shear modulus along the skirt length, Δs refers to the local displacement of the skirt soil reaction and \bar{k}_0^{skirt} is a dimensionless stiffness of the skirt soil reaction for $\alpha = 0$, as detailed in Table 3 of Suryasentana et al. (2022). Fig. 4 shows the torsional stiffness k_q^{skirt} of the skirt soil reactions estimated using G_{fac} or $G_{\text{eq}}^{\text{skirt}}$, where it is clear that using G_{fac} produce more realistic estimations. Fig. 5 summarises the steps in MWM to estimate the soil reaction stiffness for inputs into OxCaisson, where Tables 4 and 5 can be used to estimate the skirt and base soil reaction stiffness, respectively.

5 Validation

OxCaisson-MWM, which refers to the OxCaisson model coupled with the soil reaction stiffness calculated following Fig. 5, is used to estimate the static stiffness of rigid caissons in the non-layered soil cases used for calibration. Fig. 6 compares these estimations with the 3D FEA-calculated values, which shows good agreement. The average (max) deviations of the estimations from the 3D FEA calculations are 4.67% (12.95%), 1.66% (5.91%), 2.77% (13.69%) and 5.15% (16.74%) for K_V , K_Q , K_H , K_M , respectively.

OxCaisson-MWM is then used to estimate the static stiffness of rigid caissons in 15 layered soil systems that are challenging for existing simplified design models (e.g. Doherty et al. 2005; Suryasentana et al. 2022), as these models require an idealised shear modulus form (e.g. Eq. 2) to be fitted against these layered soil profiles, which is not straightforward. The first three soil profiles are layered clay soil profiles (see Fig. 7) that are representative of offshore wind sites (Burd et al. 2020). More details about these profiles can be found in Suryasentana & Mayne (2022). The remaining 12 soil profiles are three-layered soil profiles similar to those studied by Poulos (1979). Table 6 lists the values of the Young's modulus and Poisson's ratio for each soil profile. A caisson diameter D of 10m and length L of 10m is adopted for this study. Fig. 8 compares the OxCaisson-MWM estimations for

the caisson stiffness with the 3D FEA calculated values, which shows reasonably good agreement. The average (max) deviations of the estimations from the 3D FEA calculations are 6.77% (15.48%), 5.88% (12.29%), 4.02% (12.28%), 6.87% (17.57%) for K_V , K_Q , K_H , K_M , respectively. These deviations are in line with those observed in the non-layered soil cases used for calibration.

The primary purpose of OxCaisson-MWM is to provide an efficient design model to estimate the static stiffness of suction caisson foundations in layered soil conditions, which are commonplace in offshore wind sites. Unlike existing simplified design models which cannot be applied to layered soil conditions, OxCaisson-MWM is versatile and can be used for both non-layered and layered soil conditions. It is also very efficient, taking less than one second to estimate each caisson stiffness compared to 10 minutes for 3D FEA. The main limitations are that the accuracy of OxCaisson-MWM has only been validated for a finite number of layered soil conditions and for fully rigid caissons. Furthermore, OxCaisson-MWM can only be used to estimate the static stiffness at low load levels, where the soil response can be approximated as being linear elastic. Thus, the main applications of OxCaisson-MWM are for fatigue limit analysis and dynamic analysis (e.g., natural frequency calculations).

6 Conclusions

This paper presents an extension to the OxCaisson model, called OxCaisson-MWM, which can provide efficient estimates of the static stiffness of suction caissons in layered soil conditions. The MWM approach improves the estimation of the soil reactions for OxCaisson in layered soil conditions, which can then be used to calculate the static stiffness of caissons. A 3D FEA study was conducted to develop and validate this approach. The results showed that the stiffness estimates produced by OxCaisson-MWM are consistent with those from the 3D FEA study.

7 Data Availability

Some or all data, models, or code that support the findings of this study are available from the corresponding author upon reasonable request.

8 Acknowledgements

Parts of the work described here were conducted during the DPhil studies of the first author at the University of Oxford. The first author would like to thank Ørsted Wind Power for funding the DPhil studentship. Byrne is supported by the Royal Academy of Engineering under the Research Chairs and Senior Research Fellowships scheme.

References

- Atkinson, J. H. (2000). Non-linear soil stiffness in routine design. *Géotechnique* 50(5), 487–508.
- Burd, H. J., Abadie, C. N., Byrne, B. W., Houlsby, G. T., Martin, C. M., McAdam, R. A., Jardine, R.J., Pedro, A.M., Potts, D.M., Taborda, D.M., Zdravković, L., and Andrade, M.P. (2020). Application of the PISA Design Model to Monopiles Embedded in Layered Soils. *Géotechnique* 70(11): 1-55. <https://doi.org/10.1680/jgeot.20.PISA.009>
- Byrne, B.W. & Houlsby, G. T. (2003). Foundations for offshore wind turbines. *Philosophical transactions. Series A, Mathematical, physical, and engineering sciences* 361(1813), 2909–30.
- Dassault Systemes (2014). Abaqus user manual. Simula Corp., Providence, RI.
- Doherty, J. P., Houlsby, G. T. and Deeks, A. J. (2005), Stiffness of flexible caisson foundations embedded in nonhomogeneous elastic soil, *Journal of Geotechnical and Geoenvironmental Engineering* 131 (12), 1498–1508.
- Efthymiou, G. and Gazetas, G. (2018), Elastic Stiffnesses of a Rigid Suction Caisson and Its Cylindrical Sidewall Shell, *Journal of Geotechnical and Geoenvironmental Engineering* 145 (2), 06018014.
- Poulos, H. G. (1979). Settlement of single piles in non homogeneous soil. *Journal of Geotechnical Engineering Division ASCE*, 105(5), 627–641.
- Suryasentana, S. K., Byrne, B. W., Burd, H. J., and Shonberg, A. (2017). Simplified model for the stiffness of suction caisson foundations under 6DoF loading. In *Proceedings of SUT OSIG 8th International Conference*, London, UK.
- Suryasentana, S. K., Burd, H. J., Byrne, B. W., & Shonberg, A. (2022). A Winkler model for suction caisson foundations in homogeneous and non-homogeneous linear elastic soil. *Géotechnique*, 72(5), 407-423.
- Suryasentana, S. K., & Mayne, P. W. (2022). Simplified method for the lateral, rotational, and torsional static stiffness of circular footings on a nonhomogeneous elastic half-space based on a work-equivalent framework. *Journal of Geotechnical and Geoenvironmental Engineering*, 148(2), 04021182.

Table 1. Displacement boundary conditions applied to the caisson at the RP (see Fig. 1) in the 3D finite element analysis to determine the global stiffness coefficients. The value of u_0 is arbitrary. U_x, U_y, U_z refer to the displacements of the caisson along the x, y, z axes, respectively. $\Theta_x, \Theta_y, \Theta_z$ refer to the rotations of the caisson about the x, y, z axes, respectively.

	U_x	U_y	U_z	Θ_x	Θ_y	Θ_z
Rigid Axial Translation	0	0	u_0	0	0	0
Rigid Lateral Translation	0	u_0	0	0	0	0
Rigid Rotation	0	0	0	u_0	0	0
Rigid Torsion	0	0	0	0	0	u_0

Table 2. Best-fit parameters in Eq. 6 for each base soil reaction stiffness

Stiffness	b_1	b_2	b_3	b_4
k_v^{base}	0.489	27.3	5	0.691
k_q^{base}	0.076	0	0	0.055
k_h^{base}	0.237	-0.049	1	0.492
k_m^{base}	0.17	5	4	0.0714

Table 3. Best-fit parameters in Eq. 7 for each skirt soil reaction stiffness

Stiffness	m_1	m_2	m_3
k_v^{skirt}	2.27	0.21	0.71
k_q^{skirt}	1.16	0	0.89
k_h^{skirt}	1.68	0.35	0.73
k_m^{skirt}	1.52	0.35	1

Table 4. Dimensionless stiffness for the skirt soil reactions (left column) where G_{fac} and G are the local values of the factored and unfactored shear modulus, respectively. The right column shows the parameters for the dimensionless stiffness for incorporation into Equation 22 of Suryasentana et al.

(2022) i.e. $\bar{k}^{\text{skirt}} = (a_1 + a_2\nu) \left(1 - \frac{(a_3 + a_4\nu)\frac{L}{D}}{(a_5 + a_6\nu)\frac{L}{D} + 1} \right)$. These parameters are determined from Table 3 of Suryasentana et al. (2022) by setting $\alpha = 0$ (i.e. the homogeneous soil case). As $G_{\text{eq}}^{\text{skirt}}$ is not available for k_c^{skirt} , the default shear modulus values proposed by Suryasentana et al. (2022) is adopted i.e. the unfactored shear modulus value G .

Dimensionless stiffness	Soil stiffness function parameters
$\bar{k}_v^{\text{skirt}} = \frac{k_v^{\text{skirt}}}{G_{\text{fac}}}$	$a_1 = 10.8, a_2 = 14.4, a_3 = 4.2, a_4 = 5.2, a_5 = 5, a_6 = 5.8$
$\bar{k}_q^{\text{skirt}} = \frac{k_q^{\text{skirt}}}{G_{\text{fac}}D^2}$	$a_1 = 10.7, a_2 = 0, a_3 = 10.4, a_4 = 0, a_5 = 14.9, a_6 = 0$
$\bar{k}_h^{\text{skirt}} = \frac{k_h^{\text{skirt}}}{G_{\text{fac}}}$	$a_1 = 23.3, a_2 = 7.6, a_3 = 10.5, a_4 = -8.9, a_5 = 12.2, a_6 = -10.5$
$\bar{k}_m^{\text{skirt}} = \frac{k_m^{\text{skirt}}}{G_{\text{fac}}D^2}$	$a_1 = 3.8, a_2 = 1.6, a_3 = 9.55, a_4 = -3, a_5 = 13.4, a_6 = -6.8$
$\bar{k}_c^{\text{skirt}} = \frac{k_c^{\text{skirt}}}{GD}$	$a_1 = -2.4, a_2 = 8.8, a_3 = 21, a_4 = -27.4, a_5 = 21, a_6 = -26.5$

Table 5. Dimensionless stiffness for the base soil reactions (left column). The right column shows the parameters for the dimensionless stiffness for incorporation into Equation 23 of Suryasentana et al.

(2022) i.e. $\bar{k}_{\text{base}} = k_0 + \left(a_1 + \frac{a_2}{1-\nu} \right) \left(1 - \frac{1}{a_3\frac{L}{D} + 1} \right)$. These parameters are determined from Table 5 of Suryasentana et al. (2022) by setting $\alpha = 0$ (i.e. the homogeneous soil case). As $G_{\text{eq}}^{\text{base}}$ is not available for k_c^{base} , the default shear modulus values proposed by Suryasentana et al. (2022) is adopted i.e. the unfactored shear modulus value at a distance $D/2$ below the caisson base G_b .

Dimensionless stiffness	Soil stiffness function parameters
$\bar{k}_v^{\text{base}} = \frac{k_v^{\text{base}}}{G_{\text{eq}}^{\text{base}}D}$	$k_0 = \frac{2\ln(3-4\nu)}{1-2\nu}, a_1 = -0.612, a_2 = -0.715, a_3 = 5.85$
$\bar{k}_q^{\text{base}} = \frac{k_q^{\text{base}}}{G_{\text{eq}}^{\text{base}}D^3}$	$k_0 = \frac{2}{3}, a_1 = -0.289, a_2 = 0, a_3 = 28.2$
$\bar{k}_h^{\text{base}} = \frac{k_h^{\text{base}}}{G_{\text{eq}}^{\text{base}}D}$	$k_0 = \frac{4}{2-\nu}, a_1 = -0.453, a_2 = -0.646, a_3 = 12$
$\bar{k}_m^{\text{base}} = \frac{k_m^{\text{base}}}{G_{\text{eq}}^{\text{base}}D^3}$	$k_0 = \frac{1}{3(1-\nu)}, a_1 = 0.01, a_2 = -0.15, a_3 = 12$
$\bar{k}_c^{\text{base}} = \frac{k_c^{\text{base}}}{G_bD^2}$	$k_0 = \left[\frac{0.185}{1-\nu} - 0.37 \right], a_1 = 0.52, a_2 = -0.314, a_3 = 25.7$

Table 6. Young's modulus profiles for 12 three-layered soil profiles analysed in the numerical study, where each layer is assumed to be homogeneous. $E_R = 1000p_{\text{atm}}$ is the reference Young's modulus of the soil, ν is the soil Poisson's ratio, z is the depth below ground level and L is the length of the caisson skirt.

Name	ν	Normalised Young's Modulus, E/E_R		
		$z < 0.3L$	$0.3L \leq z < 0.7L$	$z \geq 0.7L$
P1	0.2	1	2	4
P2	0.2	1	4	2
P3	0.2	2	1	4
P4	0.2	2	4	1
P5	0.2	4	2	1
P6	0.2	4	1	2
P7	0.49	1	2	4
P8	0.49	1	4	2
P9	0.49	2	1	4
P10	0.49	2	4	1
P11	0.49	4	2	1
P12	0.49	4	1	2

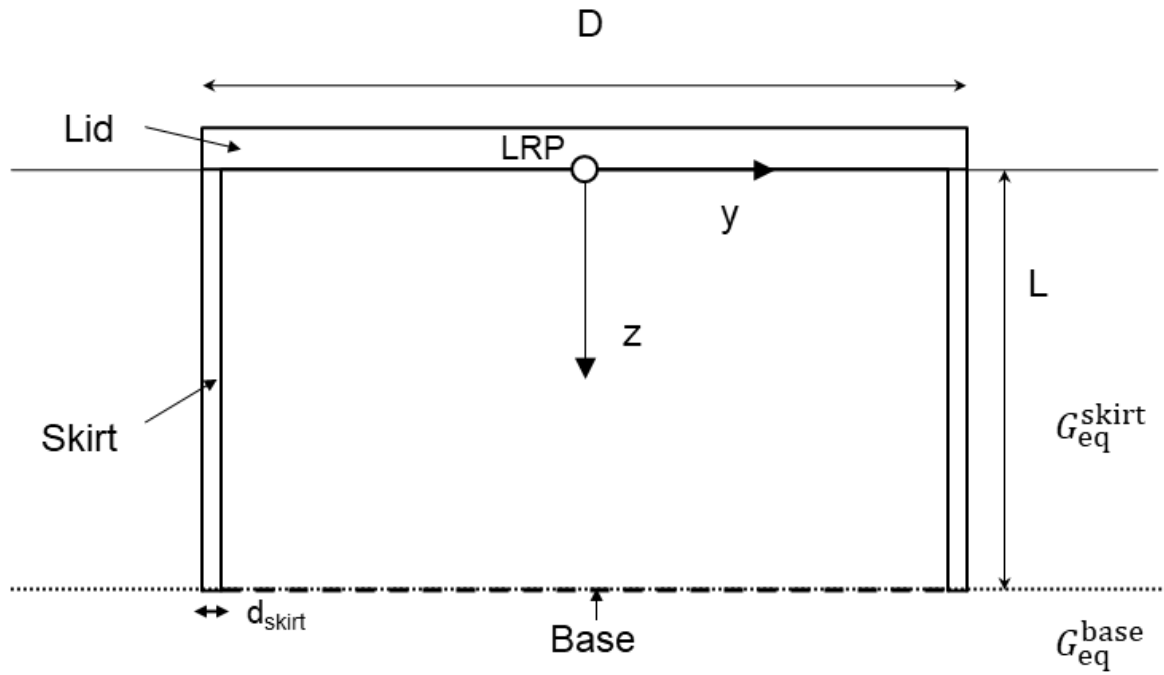


Figure 1 Schematic diagram of a suction caisson foundation of diameter D with embedded length L . The loading reference point (LRP) is at the centre of the lid base.

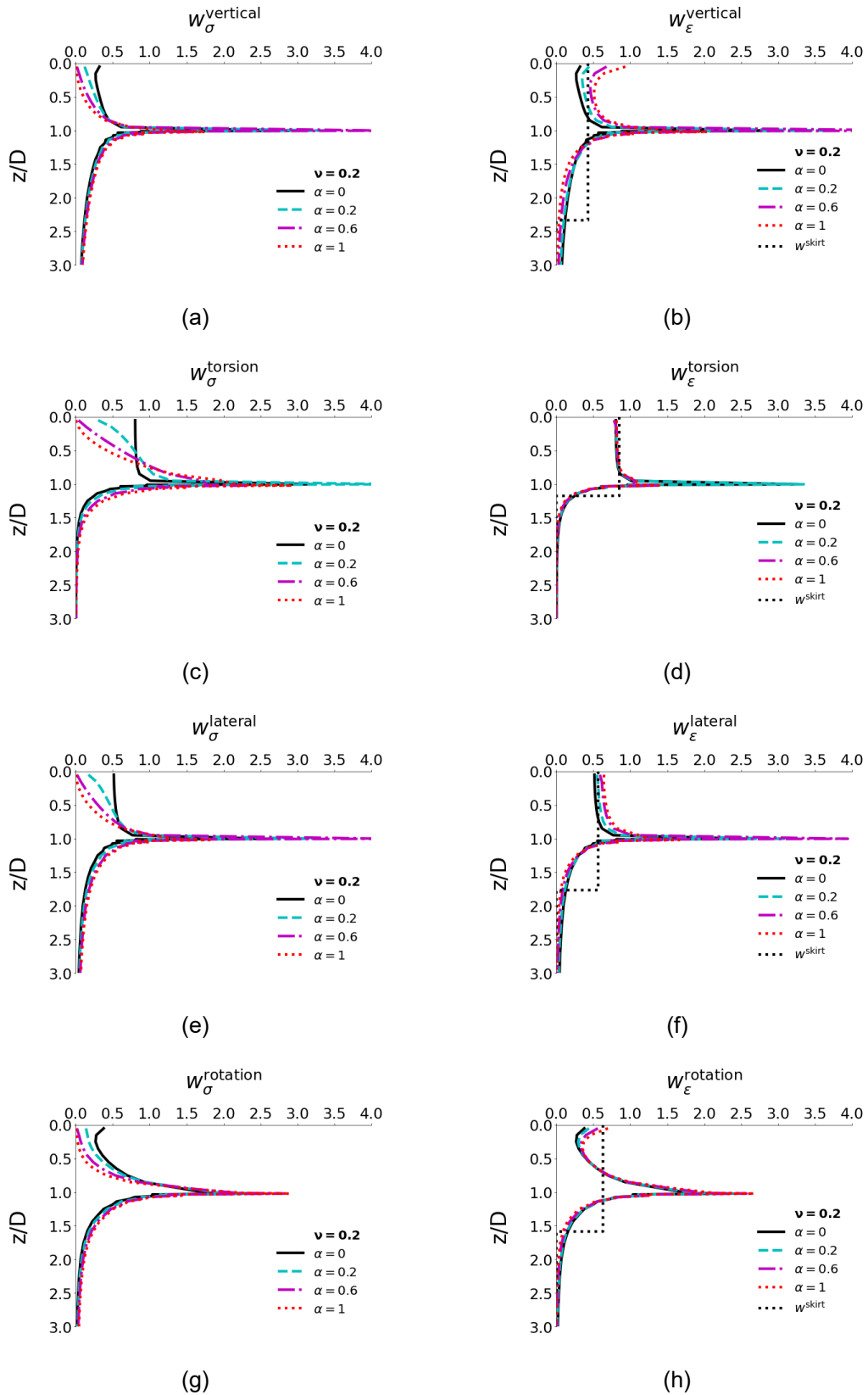


Figure 2 Comparison of w_σ and w_ϵ due to skirt soil reactions, for $L/D = 1$, $\nu = 0.2$ and $\alpha = 0, 0.2, 0.6, 1$ under the following displacements: (a), (b) Vertical (c), (d) Torsional (e), (f) Lateral (g), (h) Rotational. w^{skirt} represent the approximate weight distributions (Eq. 5) for the skirt soil reactions employing the parameters in Table 3.

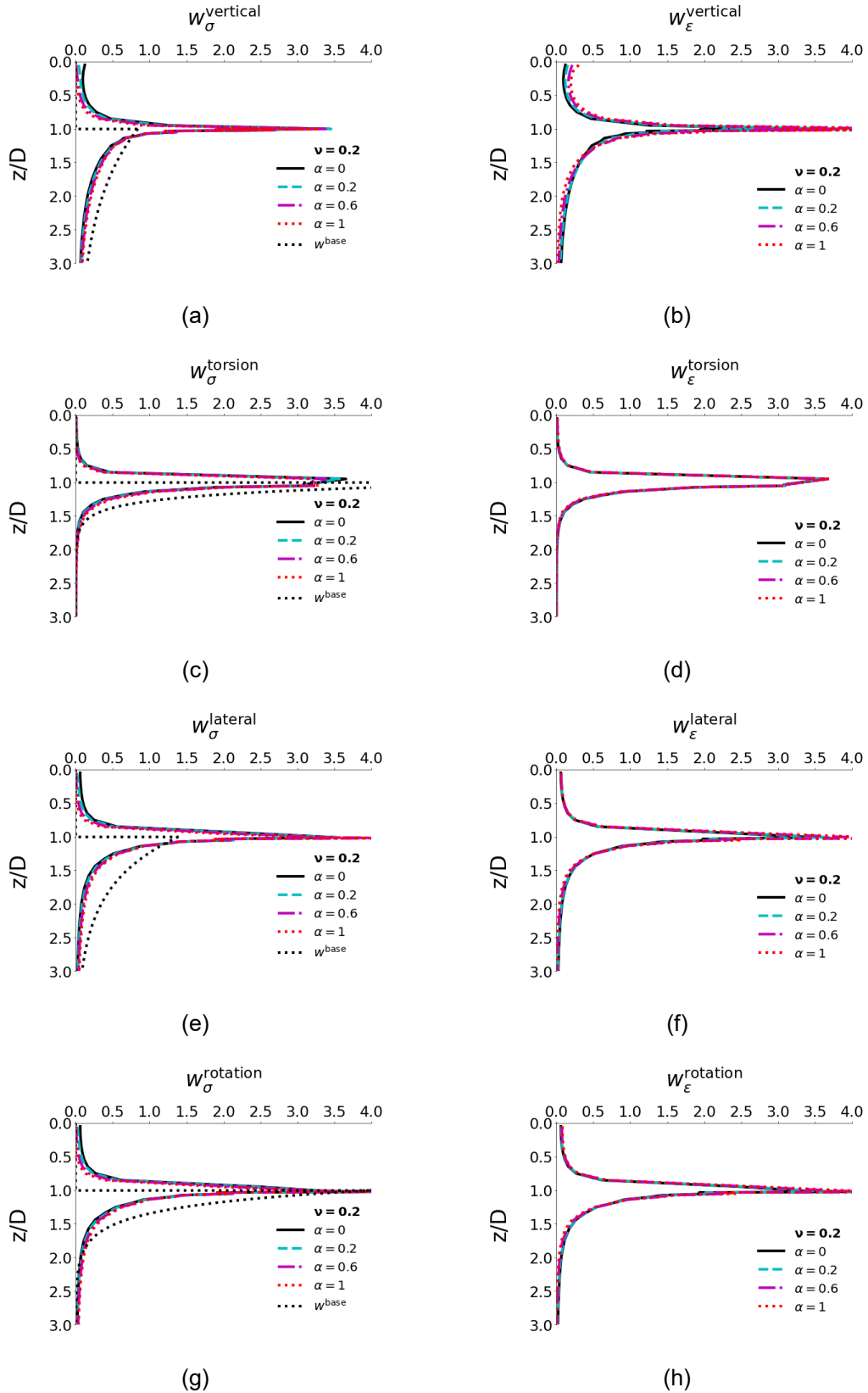


Figure 3 Comparison of w_σ and w_ϵ due to base soil reactions, for $L/D = 1$, $\nu = 0.2$ and $\alpha = 0, 0.2, 0.6, 1$ under the following displacements: (a), (b) Vertical (c), (d) Torsional (e), (f) Lateral (g), (h) Rotational. w^{base} represent the approximate weight distributions (Eq. 4) for the base soil reactions employing the parameters in Table 2.

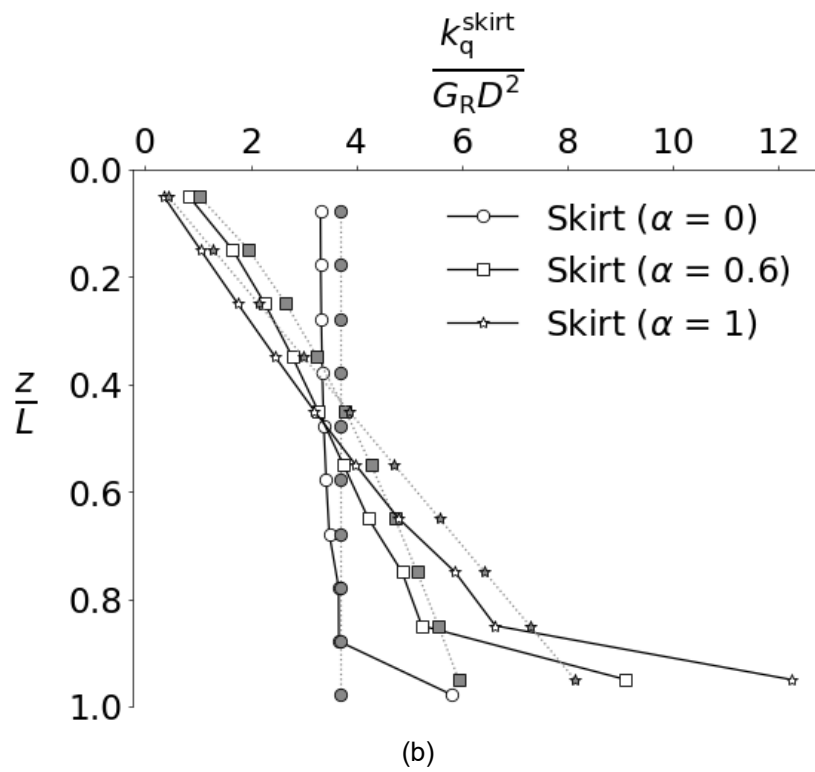
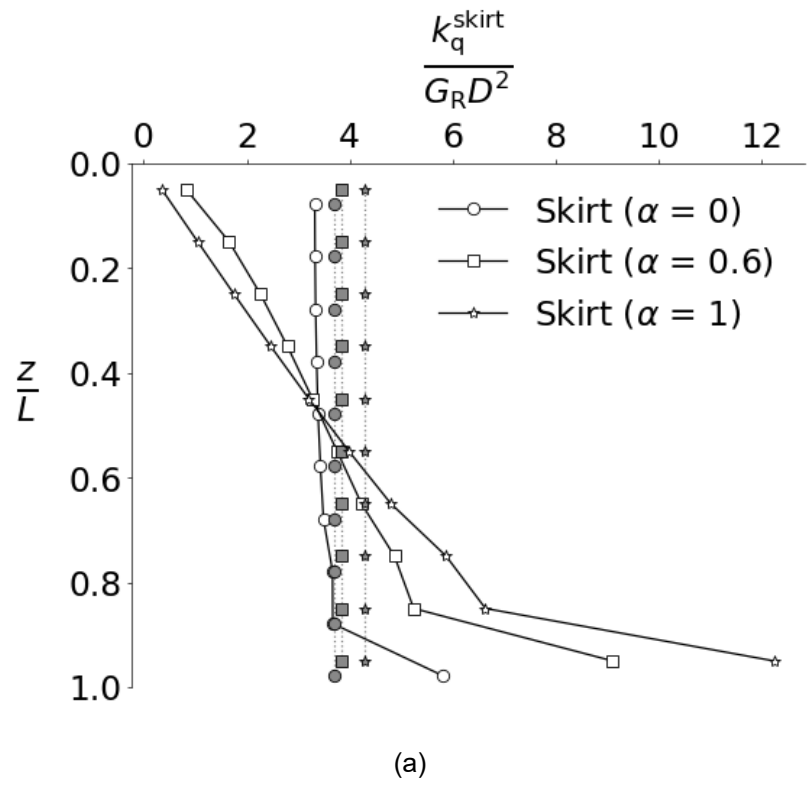


Figure 4 Comparison of the torsional stiffness of the skirt soil reactions calculated from 3D FEA (shown as white markers) with those estimated using $G_{\text{eq}}^{\text{skirt}}$ or G_{fac} (shown as grey markers), for $L/D = 1$, $\nu = 0.2$ and $\alpha = 0, 0.6, 1$. (a) The grey markers correspond to estimations using $G_{\text{eq}}^{\text{skirt}}$. (b) The grey markers correspond to estimations using G_{fac} .

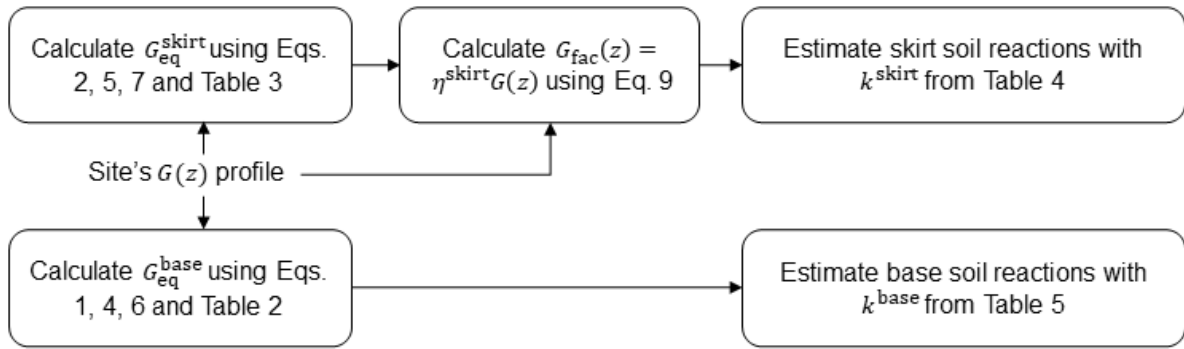


Figure 5 Flow chart showing the steps involved in MWM for estimating the soil reactions for a suction caisson foundation in a site with some shear modulus $G(z)$ profile.

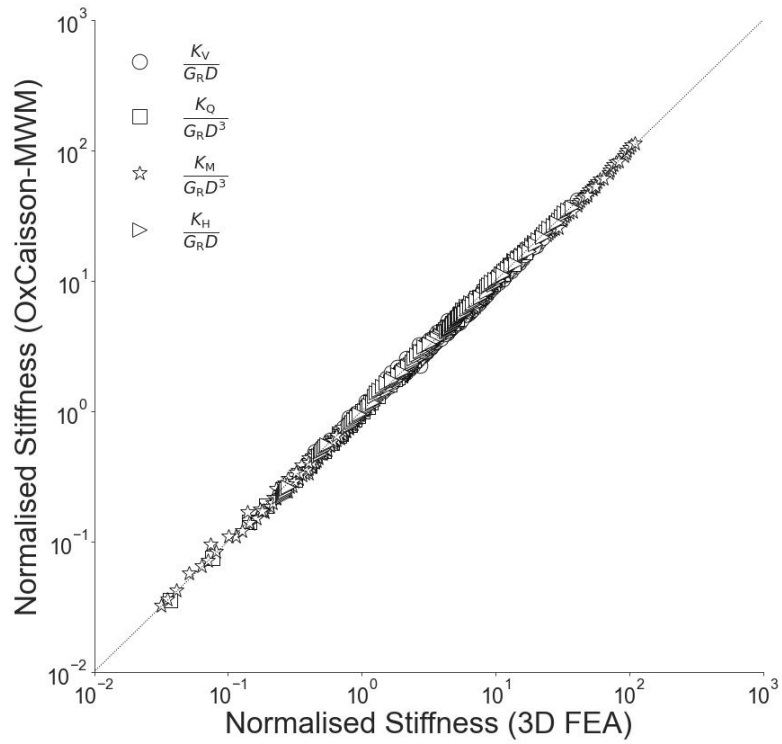


Figure 6 Comparison of the caisson stiffness estimated by Ox-Caisson-MWM with those calculated using 3D FEA for $\alpha = 0, 0.2, 0.4, 0.6, 0.8, 1$, $L/D = 0, 0.125, 0.25, 0.5, 1, 2$ and $\nu = 0.2, 0.49$. Both axes are in log scale and the dotted line is a 1:1 line.

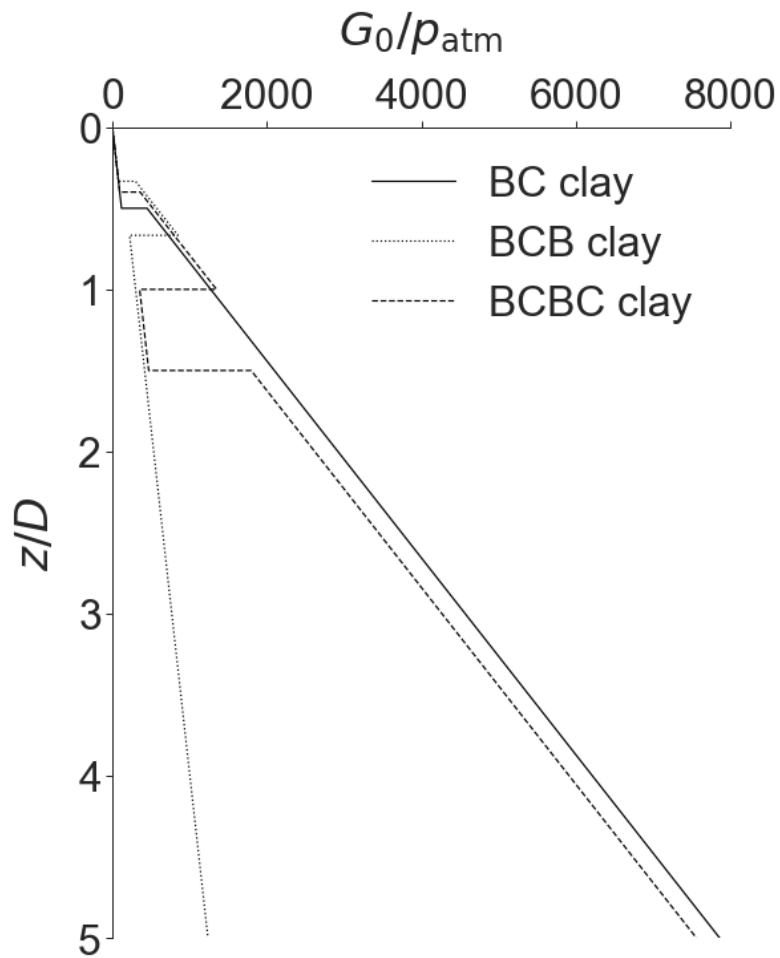


Figure 7 Comparison of the normalized initial shear modulus G_0 of the three complex soil profiles that are similar to layered soil profiles previously investigated by Burd et al. (2020) and Suryasentana & Mayne (2022), where the depth is normalized by the foundation diameter $D = 10\text{m}$. 'BC clay' comprises of Bothkennar clay overlying Cowden till, 'BCB clay' comprises of a Bothkennar clay soil matrix with an interbedded Cowden till layer and 'BCBC clay' comprises of a Cowden till soil matrix with two interbedded Bothkennar clay layers.

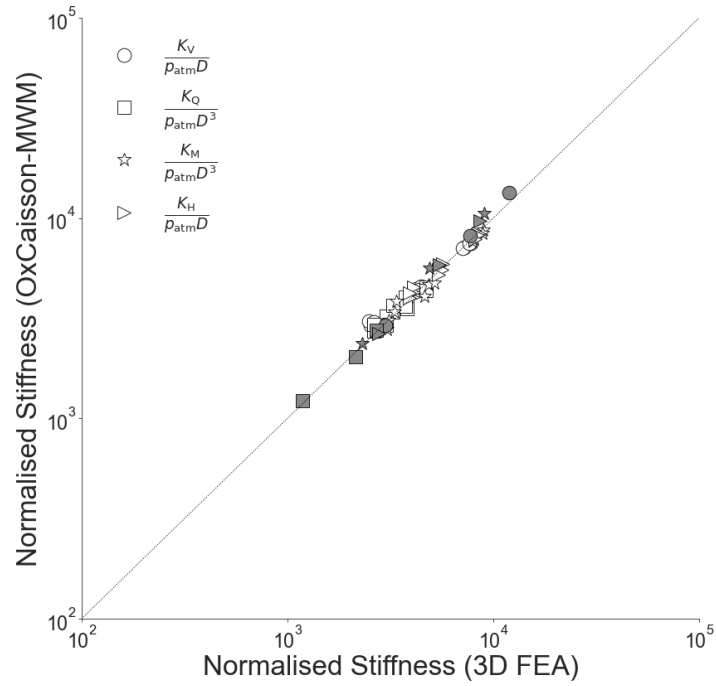


Figure 8 Comparison of the normalized caisson stiffness estimated by Ox-Caisson-MWM with the corresponding 3D FEA results, for the layered soil profiles. White markers correspond to the results for the layered soil profiles detailed in Table 6, while grey markers correspond to the results for the layered soil profiles shown in Fig. 7. Both axes are in log scale and the dotted line is a 1:1 line.